NASA Contractor Report 187539

ICASE INTERIM REPORT 16

PRELIMINARY CALIBRATION OF A GENERIC SCRAMJET COMBUSTOR

P. A. Jacobs
R. G. Morgan
R. C. Rogers
M. Wendt
C. Brescianini
A. Paull
G. Kelly

(NASA-CR-187539) PRELIMINARY CALIBRATION OF A GENERIC SCRAMJET COMBUSTOR Final Interim Report No. 16 (ICASE) 32 p   CSCL 21E

N91-21139

Unclas
G3/07 0005414

INSTITUTE FOR COMPUTER APPLICATIONS IN SCIENCE AND ENGINEERING
NASA Langley Research Center, Hampton, Virginia 23665

Operated by the Universities Space Research Association

NASA

National Aeronautics and
Space Administration

Langley Research Center
Hampton, Virginia 23665-5225

ICASE INTERIM REPORTS

ICASE has introduced a new report series to be called ICASE Interim Reports. The series will complement the more familiar blue ICASE reports that have been distributed for many years. The blue reports are intended as preprints of research that has been submitted for publication in either refereed journals or conference proceedings. In general, the green Interim Report will not be submitted for publication, at least not in its printed form. It will be used for research that has reached a certain level of maturity but needs additional refinement, for technical reviews or position statements, for bibliographics, and for computer software. The Interim Reports will receive the same distribution as the ICASE Reports. They will be available upon request in the future, and they may be referenced in other publications.

Robert G. Voigt
Director

Preliminary Calibration of a Generic Scramjet Combustor[*]

P. A. Jacobs[1], R. G. Morgan[2], R. C. Rogers[3],
M. Wendt[2], C. Brescianini[2], A. Paull[2] and G. Kelly[2]

[1]ICASE, NASA Langley Research Center,
Hampton, VA 23665, USA.

[2]Department of Mechanical Engineering,
The University of Queensland,
St Lucia, Qld 4067, AUSTRALIA.

[3]Hypersonic Propulsion Branch,
NASA Langley Research Center.

Abstract

The results of a preliminary investigation of the combustion of hydrogen fuel at hypersonic flow conditions are provided. The tests were performed in a generic, constant-area combustor model with test gas supplied by a free-piston-driven reflected-shock tunnel. Static pressure measurements along the combustor wall indicated that burning did occur for combustor inlet conditions of $P_{static} \simeq 19kPa$, $T_{static} \simeq 1080K$ and $U \simeq 3630m/s$ with a fuel equivalence ratio $\phi \simeq 0.9$. These inlet conditions were obtained by operating the tunnel with stagnation enthalpy $H_s \simeq 8.1MJ/kg$, stagnation pressure $P_s \simeq 52MPa$ and a contoured nozzle with a nominal exit Mach number of 5.5.

PRECEDING PAGE BLANK NOT FILMED

Nomenclature

f : mass fraction
H : stagnation enthalpy
M : Mach number
$\dot{m}$: mass flow
P : pressure
T : temperature
t : time
U : velocity
x : (streamwise) distance along combustor duct

γ : ratio of specific heats
ϕ : fuel equivalence ratio
ρ : density

Subscripts

$fill$: initial shock-tube filling conditions
$flight$: free-flight conditions
$pitot$: as measured with a Pitot probe
$plenum$: hydrogen plenum conditions
s : nozzle supply conditions
$static$: free-stream conditions at the nozzle exit plane

1 Introduction

The development of the National Aero-Space Plane and generic air-breathing propulsion systems for the flight regime $10 \leq M_{flight} \leq 25$ has led to a demand for experimental combustion data. So far, the only combustion experiments at the high-speed end of this regime have been performed in free-piston-driven shock tunnels [1] [2] [3] [4]. These experiments typically used a $25mm \times 51mm$ cross-section combustor of length $0.5m$.

In reference [3] it was reported that combustion of hydrogen in the $25mm \times 51mm$ combustor was achieved in the hypersonic flow at $M \simeq 5.6$ with static pressure $19kPa$, and stagnation enthalpies in the range $6MJ/kg \leq H_s \leq 13MJ/kg$. However, it was observed that the hydrogen did not burn when the combustor cross-section was increased to $49.5mm \times 51mm$. It was hypothesized that the burning in the $25mm \times 51mm$ combustor was promoted by compression and heating of the air stream by the boundary layers growing along the combustor walls. For the $49.5mm \times 51mm$ combustor, the boundary layer effects were smaller and so did not promote burning within the $0.5m$ length of that particular model.

In order to check this hypothesis, a similar experiment was conducted in a $47mm \times$

$100mm \times 1.32m$ combustor model which was geometrically similar to (but approximately double the size of) the $25mm \times 51mm$ model. The primary goal was to see if combustion occurred at distances greater than $0.5m$ along the duct. This particular experiment has also been the focus of a continuing computational study in which the transient flow in the combustor is simulated in a time accurate manner [5] [6].

The purpose of this report is to describe the combustor geometry, the data reduction procedure, and the data from some preliminary shots. These shots are 1006 through 1009 as recorded in the T4 facility logbooks. The operation of the T4 shock tunnel and the evaluation of the test flow conditions are described in Section 2. Section 3 contains contains a description of the combustor model while Section 4 describes the instrumentation and data reduction. The quasi-steady wall-pressure measurements are presented in Section 5 and a full set of time traces is included in appendix A.

2   Shock-Tunnel Operation

The principal features of a free-piston driven shock tunnel, along with an approximate wave diagram, are shown in Fig. 1. The driver tube, which initially contains low pressure helium downstream of the piston, and the shock tube which contains the test gas, are separated by the primary diaphragm. Attached to the downstream end of the $75mm$ diameter shock tube is the facility nozzle with a throat diameter of $25mm$. The subsonic portion of the nozzle effectively closes the downstream end of the shock tube and forms the shock reflection region. The test gas is retained in the shock tube by a thin mylar diaphragm. The supersonic portion of the nozzle empties directly into a test section and dump tank which is evacuated to approximately $30Pa$. The inlet of the combustor model is located close to the exit plane of the contoured nozzle which has a nominal exit Mach number of 5.5.

The first stage of operation is the launch of the piston and its acceleration along the compression tube. The driving force is supplied by compressed air from a reservoir. The helium in front of the piston is compressed and eventually bursts the primary diaphragm (at a pressure $56.6MPa$ for a $4mm$ thick diaphragm). After diaphragm rupture, the helium expands into the shock tube and shock-compresses the test gas before it. The *primary* shock wave travels the length of the shock tube, reflects from the closed end, and brings the test gas to rest in the nozzle supply region. Operation in this manner is called *tailored* and is shown in the wave diagram (Fig. 1(b)) by the contact surface coming to rest when intercepted by the reflected shock. Ideally the nozzle supply conditions, characterized by the stagnation enthalpy H_s and pressure P_s, are maintained as the reflected shock continues
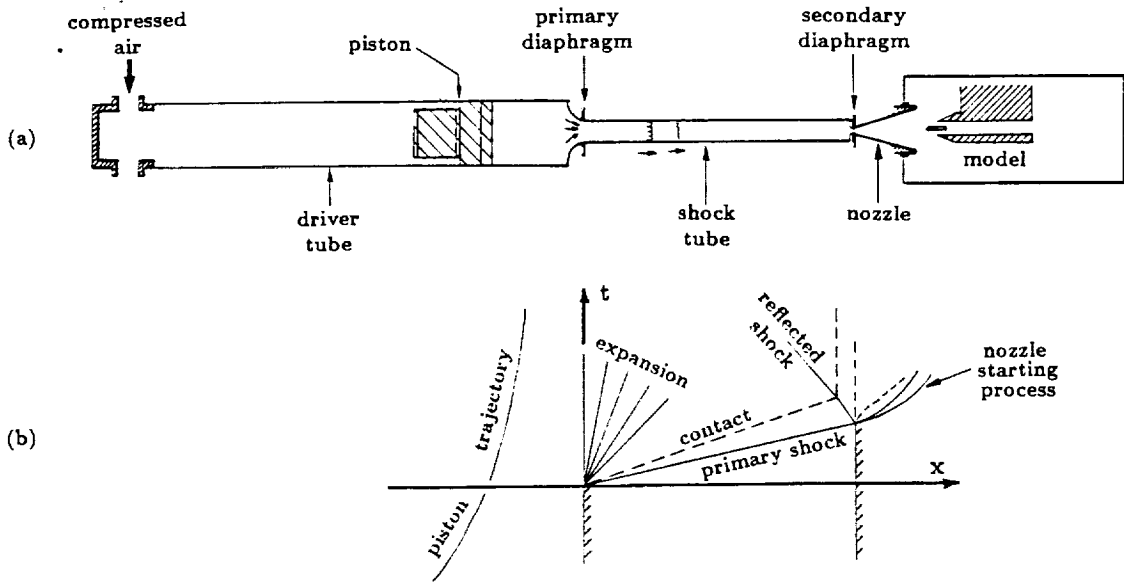
Figure 1: Reflected-shock tunnel operation. (a) Tunnel schematic, (b) $x - t$ wave diagram.

upstream though the driver gas. In an effort to delay the arrival of the driver gas at the nozzle throat and increase the available test time, the shock tube was operated in an *undertailored* mode where the reflected shock accelerates into the driver gas and an expansion propagates into the nozzle supply region. This mode of operation increases the distance between the driver-gas/test-gas interface and the end wall of the shock tube but also results in an unavoidable drop in P_s shortly after shock reflection. The net result is a typical nozzle supply pressure history as shown in Fig. 2. The transducer used to obtain this trace was located approximately 8 centimetres upstream of the closed end of the shock tube. Hence, the passage of the primary and reflected shocks are shown as distinct events. Because of the location and limited response time for the transducer, the peak reflection pressure was not recorded. Once past the maximum value, P_s continued to decay due to the combined effects of undertailored operation and driver dynamics. For pure helium driver gas and the operation considered here, this decay was typically $25 - 30\%$ during a nominal $0.5ms$ test time.

Upon shock reflection, the light secondary diaphragm bursts and some of the test gas following the primary shock expands through the nozzle throat into the divergent part of the nozzle. The nozzle then expands the hot test gas to a parallel and uniform test flow at
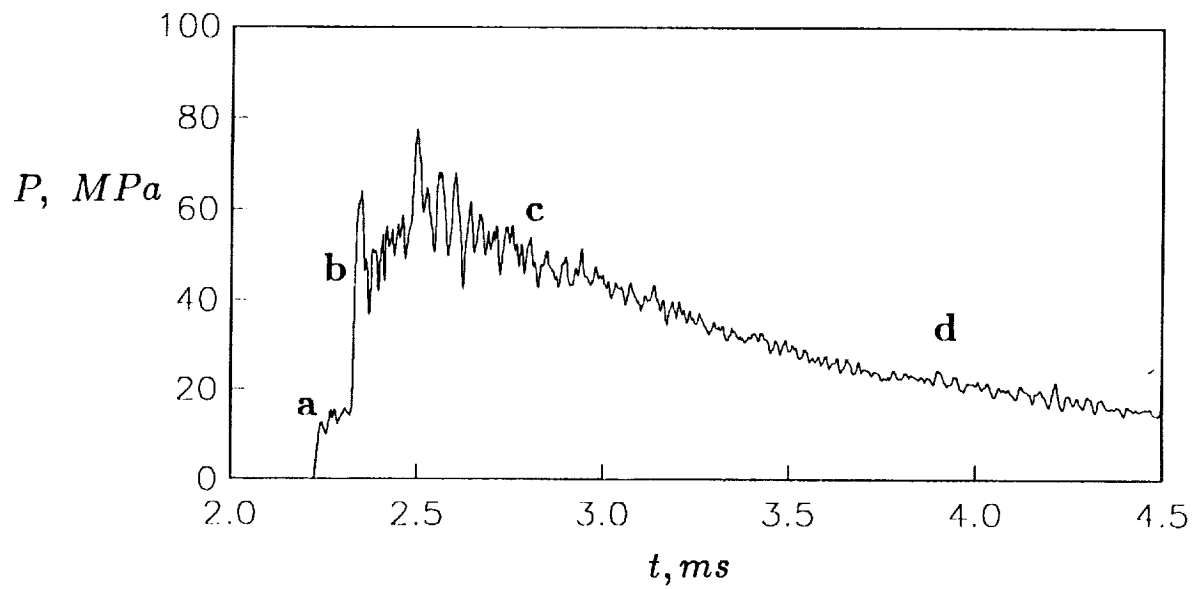
3

Figure 2: Typical history of the (unfiltered) nozzle supply pressure showing the principal events: (a) arrival of the incident shock; (b) reflected shock; (c) establishment of equilibrium pressure; (d) driver gas contamination.

the inlet to the combustor.

2.1 Test Flow Conditions

The only flow property measured in the test region (at the exit plane of the nozzle) was Pitot pressure. Other flow properties were inferred using quasi-one-dimensional computer codes and the following procedure. Note that measurements from shot 1006 have been used as the basis for the following discussion.

Step 1: The shock tube was initially filled with air at $P_{fill} = 163.5kPa$ and $T_{fill} = 296K$. The passage of the primary shock was recorded at 3 locations (spacing $2.005m$) by a set of coupled pressure transducers. An average shock speed between stations 2 and 3 was estimated as $3000m/s$ but, because the primary shock weakened as it traveled along the shock tube, there is a $\pm 10\%$ uncertainty in this estimate.

Step 2: The nozzle supply conditions (behind the reflected shock) were estimated with the FORTRAN program "ESTC" [7] which incorporated an equilibrium-chemistry model for air. From the shock reflection conditions, the under-tailored operating conditions allowed the gas to expand adiabatically (and in chemical equilibrium) to the measured nozzle supply pressure of $P_s \simeq 52MPa \pm 10\%$. This expansion resulted in an estimated stagnation enthalpy $H_s \simeq 8.1MJ/kg$ and stagnation temperature $T_s \simeq 5280K$. Note that a 10% uncertainty in shock speed introduces a 15% uncertainty in H_s and a 10% uncertainty in T_s.

Step 3: Using these stagnation conditions, the flow at the exit plane of the nozzle was estimated with the quasi-one-dimensional program "NENZF" [8] in which the test gas consisted of a mixture of the species N_2, N, O_2, O, NO, Ar, NO^+ and e^-. The gas was assumed to be in chemical equilibrium at the nozzle throat but a finite rate chemistry model with 11 reactions was used in the expansion region of the nozzle. The calculation was continued along the nozzle until the computed pitot pressure (calculated as $0.92\rho U^2$) was equal to the measured pitot pressure ($P_{pitot}/P_s = 0.014$). The *quasi-steady* conditions at the end of the nozzle (and inlet to the combustor) are shown in Table 1. The uncertainties listed in the table were obtained from an estimate of the flow conditions for a primary shock speed of $3300m/s$.

3   The Scramjet Combustor Model

The combustor model used in this experiment is the same as that used in the pressure-scaling study [9] except for the first $120mm$ of the duct. Detailed drawings of the model components

Flow Quantity	Value	Uncertainty %
P_{static}	$19 kPa$	12
ρ	$6.03 \times 10^{-2} kg/m^3$	8
T_{static}	$1080 K$	21
U	$3630 m/s$	6
M	5.6	3
$\gamma - 1$	0.334	3
f_{N_2}	0.7228	-
f_N	0	-
f_{O_2}	0.1914	3
f_O	0.0051	100
f_{NO}	0.0665	-
f_{Ar}	0.0129	-
f_{NO+}	0	-
f_{e-}	0	-

Table 1: Test flow conditions at the nozzle exit plane.

are available in [10].

An schematic view of the model is shown in Fig. 3. The combustor duct consisted of upper and lower walls (starting at $x = 0$ and extending to $x = 1.32m$) and two sidewalls which are not shown in the figure. The inlet cross-section was $47.14mm$ high by $100mm$ across and remained constant for the length of the duct. Fuel was added to the air flow via a centrally located injector strut which protruded forward from the duct inlet by $138mm$. This distance was specified so that the shock propagating from the strut leading edge (and the subsequent expansion) did not enter the combustor duct. The strut spanned the duct and fuel was added to the air stream as a coflowing jet at $x = 0.113m$. All leading edges are sharp.

The geometry was intended to produce a nominally two-dimensional flow so that interpretation of wall pressure measurements and CFD analysis would be relatively simple. However, there are a number of factors which introduce uncertainty. The inlet to the model was located $0.07m$ downstream of the nozzle exit plane (nozzle length $\simeq 0.82m$) and the test flow nonuniformities are not well known. Also, fences were not used along the protruding section of the injector strut.

The fuel system is similar to that reported in [2]. A fixed volume ($V = 1.81 \times 10^{-3}m^3$) consisting of a small reservoir and a Ludwig tube initially contains hydrogen at room temper-
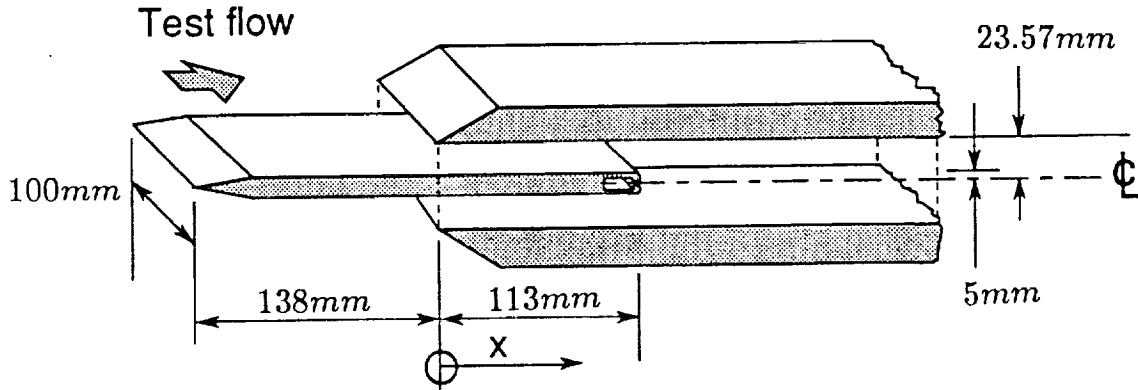
6

Figure 3: Schematic view of the $47mm \times 100mm \times 1.32m$ combustor duct.

ature and at a pressure of approximately $1MPa$. This volume is isolated from the injector plenum by a *fast-acting* valve [11] which is activated (from the tunnel recoil) some time before the air flow arrives in the test section. Timing sequences are set so that the fuel flow through the injector is established several milliseconds before the air flow. There is a circular-arc throat at the exit of the injector with a height of $1.45mm$ and a span of $97mm$ (across the combustor duct). Note that these dimensions are slightly different to the original dimensions given in [10]. Sonic conditions should exist at the throat during a run and stagnation pressure of the hydrogen is measured by two PCB pressure transducers in the plenum between the fast-acting valve and the injector throat. The fuel system has been calibrated and provides a mass flow of hydrogen given by

$$\dot{m}_{H2}[kg/s] = 6.67 \times 10^{-5} \; P_{plenum}[kPa] \; (\pm 5\%) \; . \tag{1}$$

4 Instrumentation

The combustor duct was instrumented with wall pressure transducers mounted along the upper wall as shown in Fig. 4. Although centerline tappings were used in this initial study,

7
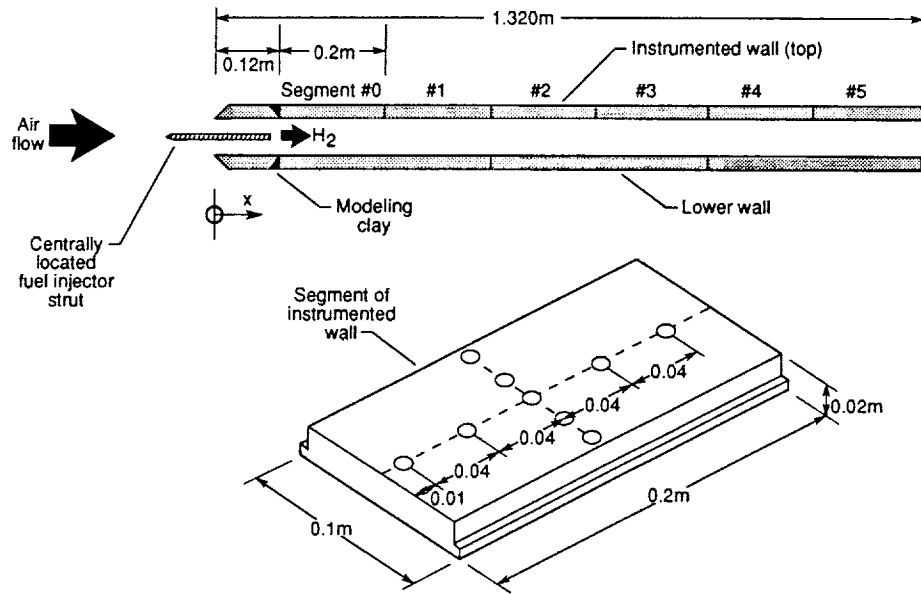
Figure 4: Layout for combustor instrumentation.

the upper-wall segments included tappings off the centerline. Table 2 shows the locations
of the wall pressure transducers. The sensitivities specified in the table are those that were
used to convert the recorded voltages to the pressures presented in Section 5.

A shortage of transducers resulted in a number of tappings being plugged for this exper-
iment. Also, space constraints resulted in the use of transducers, for $0.33m \leq x \leq 0.81m$,
which were not *acceleration compensated* and not as sensitive as the preferred PCB112 trans-
ducers. In hindsight, this was not a good idea as the signals from these transducers were
very poor.

Initial shots indicated that stress-waves in the model severely degraded the pressure sig-
nals. The transmission of these waves was reduced in the shots reported here by chamfering
the trailing edge of the first segment $(0 \leq x \leq 0.12m)$ of the duct wall (see Fig. 4) and
filling the gap with modelling clay. This arrangement effectively isolated the instrumented
wall from the impact of the facility starting flow.

Analysis of the recorded pressure signals included filtering each with a *moving average*
filter (averaging over a window of $0.05ms$) and then normalizing by the filtered nozzle supply
pressure. This normalization procedure was an attempt to remove some of the transient
aspects of the test flow (specifically the long term decay in P_s after the peak) and was

8

Wall Segment	x (m)	data-box Module	transducer type (PCB)	Serial #	Sensitivity (mV/kPa)	Δt (ms)	Comment
0	0.130	1	112A	2540	6.82	0.270	
	0.170	2	112A2	2542	7.20	0.281	bad for shot 1008
	0.210	3	112A2	2539	6.78	0.292	
	0.250	4	112	2535	6.70	0.303	
	0.290	5	112	2538	7.06	0.314	
1	0.330	6	105A2	341	0.598	0.324	bad
	0.370	12	105A2	352	0.908	0.335	
	0.410	8	105A	368	0.253	0.346	consistently high
	0.450	-	-	-	-	-	
	0.490	9	105A	369	0.705	0.368	
2	0.530	10	105A	359	0.374	0.378	
	0.570	-	-	-	-	-	
	0.610	11	105A	371	0.546	0.400	bad
	0.650	-	-	-	-	-	
	0.690	7	105A12	364	0.780	0.422	
3	0.730	13	105A	363	0.353	0.342	
	0.770	-	-	-	-	-	
	0.810	14	105A	346	0.633	0.354	high for 1009
	0.850	-	-	-	-	-	
	0.890	15	112A	4902	6.54	0.476	
4	0.930	16	112A	2541	6.86	0.486	
	0.970	-	-	-	-	-	
	1.010	17	112A	4903	6.79	0.508	
	1.050	-	-	-	-	-	
	1.090	18	112A	2543	6.98	0.530	
5	1.130	-	-	-	-	-	
	1.170	19	113A	3384	2.80	0.551	
	1.210	-	-	-	-	-	
	1.250	20	112A	2534	5.84	0.573	bad for 1009
	1.290	-	-	-	-	-	
Pitot	0.0	21	111A	1936	0.151	0.235	

Table 2: Transducer positions and specifications.

Data-box	Time Interval (ms)			
Module	shot 1006	1007	1008	1009
1	3.0-3.2	3.0-3.2	3.0-3.2	-
2	3.0-3.3	3.2-3.5	-	3.7-4.0
3	3.0-3.1	2.9-3.1	2.9-3.1	3.7-4.0
4	3.3-3.6	3.4-3.7	3.2-3.5	3.7-4.0
5	3.3-3.6	3.4-3.7	3.2-3.5	3.7-4.0
12	3.2-3.5	3.3-3.6	3.2-3.5	3.5-3.8
8	3.2-3.5	3.4-3.7	3.2-3.5	3.5-3.8
9	3.3-3.6	3.4-3.7	3.4-3.7	3.7-4.0
10	3.2-3.5	3.4-3.7	3.4-3.7	3.7-4.0
7	3.3-3.6	3.5-3.8	3.4-3.7	3.6-3.9
13	3.3-3.6	3.5-3.8	3.4-3.7	3.7-4.0
14	3.3-3.6	3.9-4.2	3.4-3.7	3.9-4.2
15	3.6-3.9	3.9-4.2	3.4-3.7	3.9-4.2
16	3.7-4.0	3.9-4.2	3.7-4.0	3.8-4.1
17	3.7-4.0	3.9-4.2	3.7-4.0	3.8-4.1
18	3.7-4.0	3.9-4.2	3.7-4.0	3.8-4.1
19	3.7-4.0	3.9-4.2	3.7-4.0	3.8-4.1
20	3.8-4.1	3.9-4.2	3.7-4.0	-

Table 3: Start and finish times for the quasi-steady sampling periods.

implemented as

$$P_{norm} = \frac{P(t)}{P_s(t - \Delta t)} \quad , \tag{2}$$

where Δt (given in Table 2) was based on an average velocity of $3700 m/s$ from the nozzle supply region to each particular transducer position. Once normalized, a quasi-steady value was evaluated as an average of the trace over a test interval which started after the passage of the starting transients (and other glitches). The start and finish times for these sampling intervals are specified for each trace in Table 3. Because the traces were unusually noisy, the test intervals were restricted to the range $0.1ms - 0.3ms$.

5 Results

Four shots were used as the basis of this experiment. These were shots

- 1006 : Hydrogen fuel injected into air test gas.

- 1007 : Hydrogen fuel injected into air test gas.

x (m)	$P/P_s \times 10^4$ shot 1006	1007	1008	1009
0.13	2.352	2.362	1.817	-
0.17	4.618	5.038	-	4.072
0.21	3.002	2.946	2.896	3.468
0.25	3.415	3.421	1.820	2.000
0.29	3.199	3.280	2.371	3.017
0.37	3.981	4.668	3.802	5.043
0.41	-	-	-	-
0.49	1.976	2.187	1.808	2.704
0.53	4.255	5.691	2.897	3.487
0.69	7.507	6.756	4.169	3.726
0.73	8.249	8.790	4.881	4.645
0.81	5.712	7.585	4.851	-
0.89	4.142	3.406	2.970	3.355
0.93	6.274	7.493	2.781	4.305
1.01	6.820	5.124	4.808	3.619
1.09	7.517	7.625	5.094	5.663
1.17	6.548	5.852	5.096	6.139
1.25	8.992	8.740	3.434	-

Table 4: Quasi-steady normalized pressures.

- 1008 : Hydrogen fuel injected into Nitrogen test gas.

- 1009 : Air test flow only, no fuel injection.

Fuel injection for shot 1008 had a mass flow of $2.074 \times 10^{-2} kg/s$ with a plenum pressure of $P_{plenum} = 311 kPa$. Fuel fuel flow rates for shots 1006 and 1007 were similar. For the air flow conditions given in Table 1, this fuel flow rate corresponds to a fuel equivalence ratio

$$\phi = 8\frac{\dot{m}_{H2}}{\dot{m}_{O2}} \simeq 0.9 \ . \tag{3}$$

The key result of this study is the set of quasi-steady wall pressure measurements shown in Fig. 5. These normalized pressure values are also given in Table 4. Superimposed on each data set is the computed wall pressure for shot 1009. The computation was performed with a Parabolized-Navier-Stokes code [12] and started at the base of the injector strut $x = 0.113m$ with air flow conditions $U = 3674m/s$, $P_{static} = 21.4kPa$, $T_{static} = 1162K$, $f_{N2} = 0.7686$ and $f_{O2} = 0.2314$. There was no fuel injection and the strut base was assumed to be a solid wall.

The pressure distributions indicate that there is a strong wave pattern present in the duct for each of these shots. The comparison between the computed pressure distribution

11
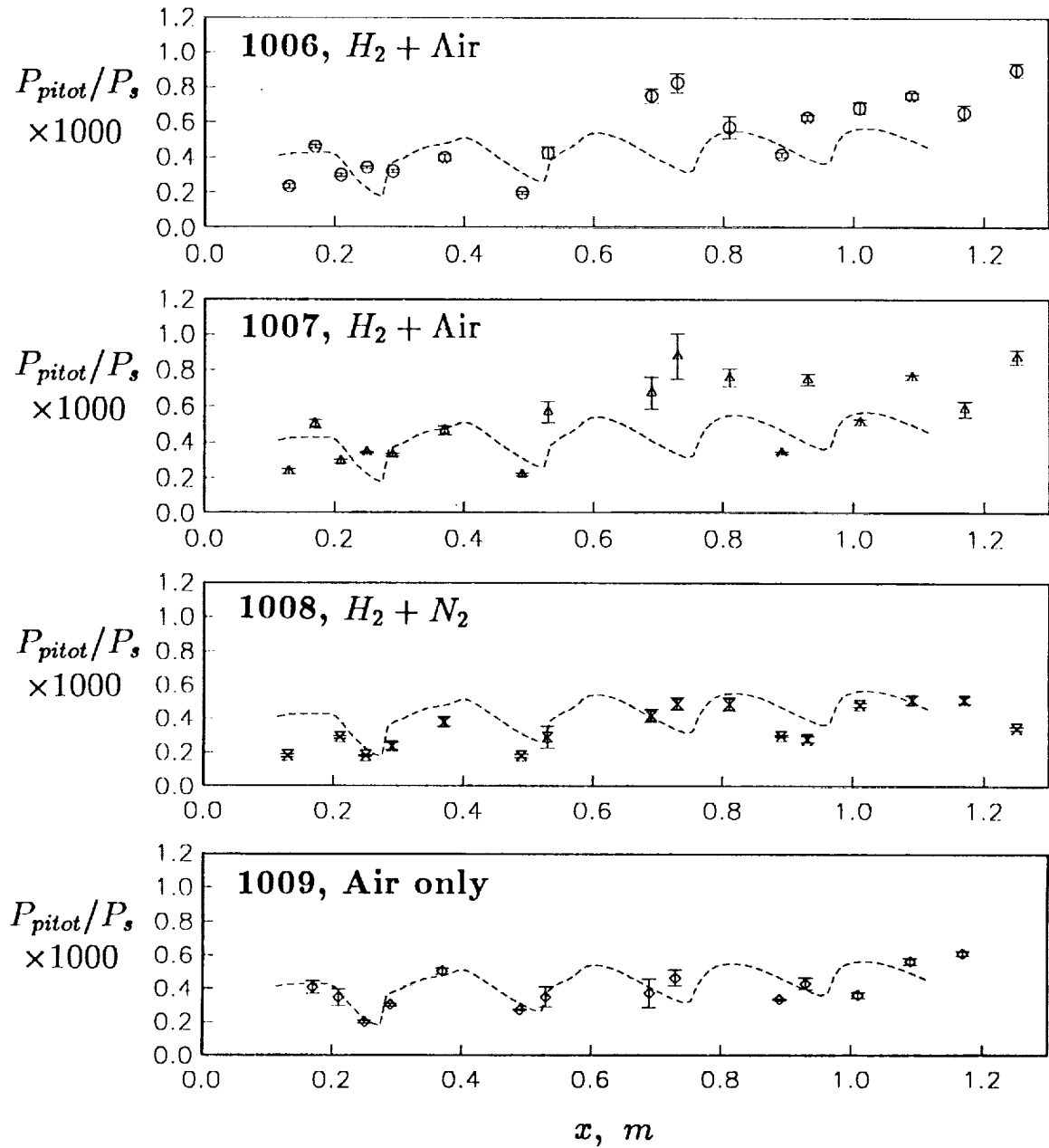
Figure 5: Quasi-steady normalized pressures along the combustor wall. The dashed line in each frame indicates the pressure distribution for a no-fuel shot (1009).

12

and the experimental distribution for shot 1009 is reasonable only for $x < 0.6m$. Although the general trend (i.e. no overall pressure rise) continues to agree for $x > 0.7m$, the wave patterns diverge beyond this location. The comparison for shot 1008, with the inclusion of a nonreacting fuel jet, is slightly worse. Confounding effects include: nonuniformities in the inflow conditions; modelling of only part of the combustor duct ($x \geq 0.113m$); and the difficulty of modelling recirculating regions with a PNS calculation.

The strong wave pattern in each distribution accounts for the relatively large pressure fluctuations along the duct but burning of the fuel can be inferred from the increased pressures shown in shots 1006 and 1007 at x locations greater than $0.6m$. (Recall that the computed pressure distribution is for a no-fuel condition.) Boundary layer growth along the duct wall and mixing effects are eliminated from the possible causes of this pressure rise as no significant pressure rise is seen in either shot 1009 or 1008 respectively. Unfortunately the transducer spacing is so large that the wave patterns are not well resolved.

6   Conclusions

This experiment demonstrated the combustion of hydrogen in a hypersonic air stream in a $47mm \times 100mm \times 1.32m$ constant area combustor duct. The pressure rise attributed to combustion was observed to begin downstream of $x = 0.6m$. Thus, this experiment provides supporting evidence for the hypothesis that combustion seen in the $25mm \times 51mm \times 0.5m$ duct (but not in the $49.5mm \times 51mm \times 0.5m$ duct) used in a previous experiment [3] was probably induced by boundary layer effects.

The data may also be useful for calibration of CFD codes and turbulence models. However, it is realized that both the resolution and quality of the pressure distributions can be improved.

Acknowledgements

References

[1] R. J. Stalker and R. G. Morgan. Parallel hydrogen injection into a constant area high enthalpy flow. *A.I.A.A. Journal*, 20(10):1468–1469, 1982.

[2] R. J. Stalker and R. G. Morgan. Supersonic hydrogen combustion with a short thrust nozzle. *Combustion and Flame*, 57:55–70, 1984.

[3] R. G. Morgan, A. Paull, R. J. Stalker, P. A. Jacobs, N. Morris, I. Stringer, and C. Brescianini. Shock tunnel studies of scramjet phenomena. NASA Contractor Report 181721, 1988.

[4] R. G. Morgan, G. A. Wallace, R. J. Stalker, N. Gottschall, R. Casey, P. A. Jacobs, C. Brescianini, G. Allen, Y. He, S. Sanderson, J. M. Simmons, G. Kelly, R. Krek, K. Skinner, C. Stacey, A. Paull, and A. Neely. Shock tunnel studies of scramjet phenomena. Supplement 4. Department of Mechanical Engineering Report, The University of Queensland, 1989.

[5] P. A. Jacobs, R. C. Rogers, E. H. Weidner, and R. D. Bittner. Flow establishment in a generic scramjet combustor. AIAA Paper 90-2096, 1990.

[6] R. C. Rogers and E. H. Weidner. Scramjet mixing establishment times for a pulse facility. AIAA Paper 91-0229, 1991.

[7] M. K. McIntosh. Computer program for the numerical calculation of frozen and equilibrium conditions in shock tunnels. Technical report, Australian National University, 1968.

[8] J. A. Lordi, R. E. Mates, and J. R. Moselle. Computer program for the numerical solution of nonequilibrium expansions of reacting gas mixtures. NASA Contractor Report 472, 1966.

[9] P. A. Jacobs and R. J. Stalker. Preliminary data for the T4 pressure-scaling experiment. Department of Mechanical Engineering Report in preparation, University of Queensland, 1990.

[10] P. A. Jacobs. A scramjet model for pressure scaling studies. Department of Mechanical Engineering Report 2/89, University of Queensland, 1989.

[11] R. G. Morgan and R. J. Stalker. Fast acting hydrogen valve. *Journal of Physics. E. Scientific Instruments.*, 16:205–207, 1983.

[12] C. P. Brescianini, R. G. Morgan, and R. J. Stalker. Numerical modeling of sidewall injected scramjet experiments in a high enthalpy airflow. *A.I.A.A. Journal of Propulsion and Power*, submitted.

A Pressure Histories

The pressure histories for each shot are summarized on three pages. The first page shows the stagnation pressure traces, the pitot pressure trace, the normalized pitot pressure trace and the shock speed trace. The second page shows the filtered wall pressures, and the third page shows the normalized wall pressure traces.

The nozzle supply pressure is taken from the largest of the two P_s traces where the trace has settled to an equilibrium value, just after the peak. The larger trace is used since heat transfer into the gauges tended to reduce their output signal when the thermal protection was damaged. The shock speed is inferred from the time taken for the primary shock to pass 3 instrumented stations in the shock tube. The distance between adjacent stations is $2.005m$.

T4 shot 1006, Straight Combustor 100mm x 47mm

Filtered P_s: solid=#22, dash=#23

Filtered Pitot Pressure #21

Normalized Pitot Pressure #21/#22
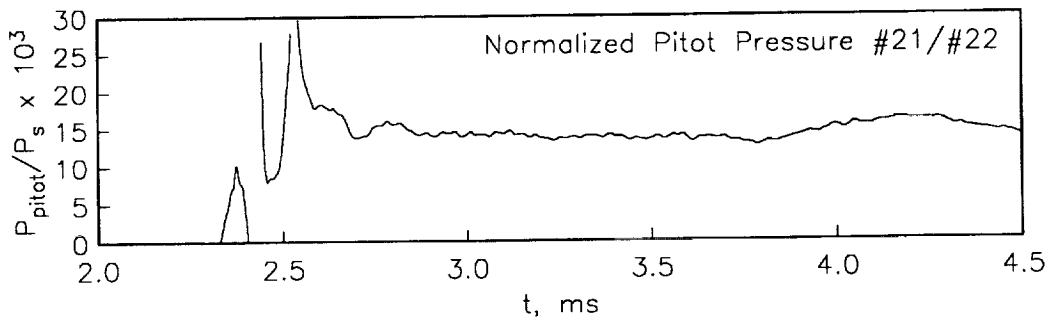
Unfiltered Shock Speed Trace #24

Filtered Wall Pressures, shot 1006

18
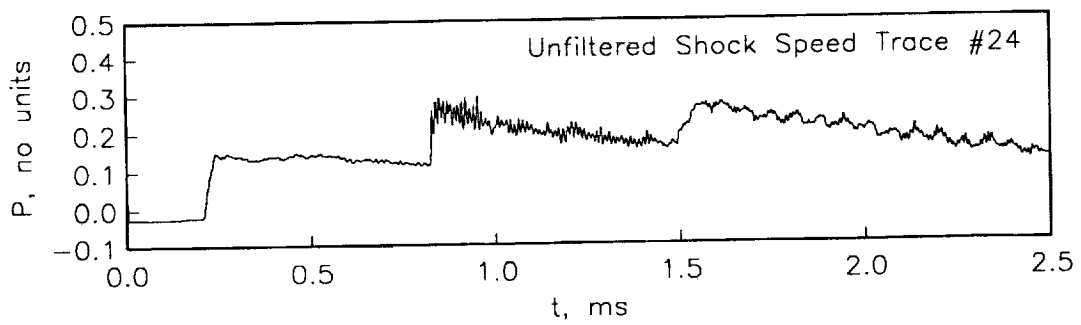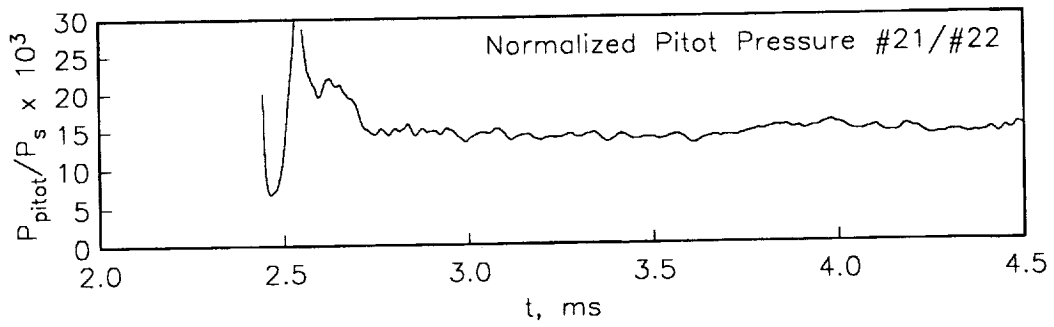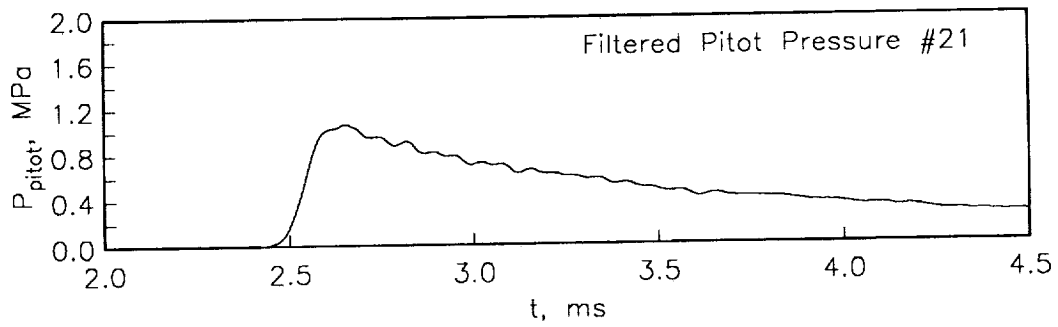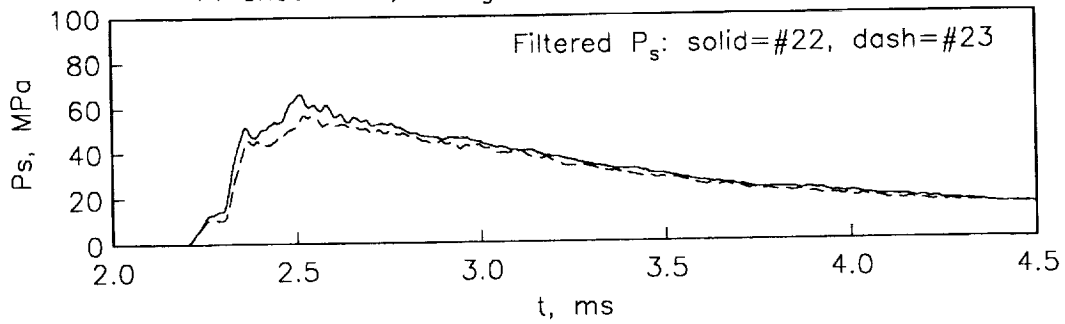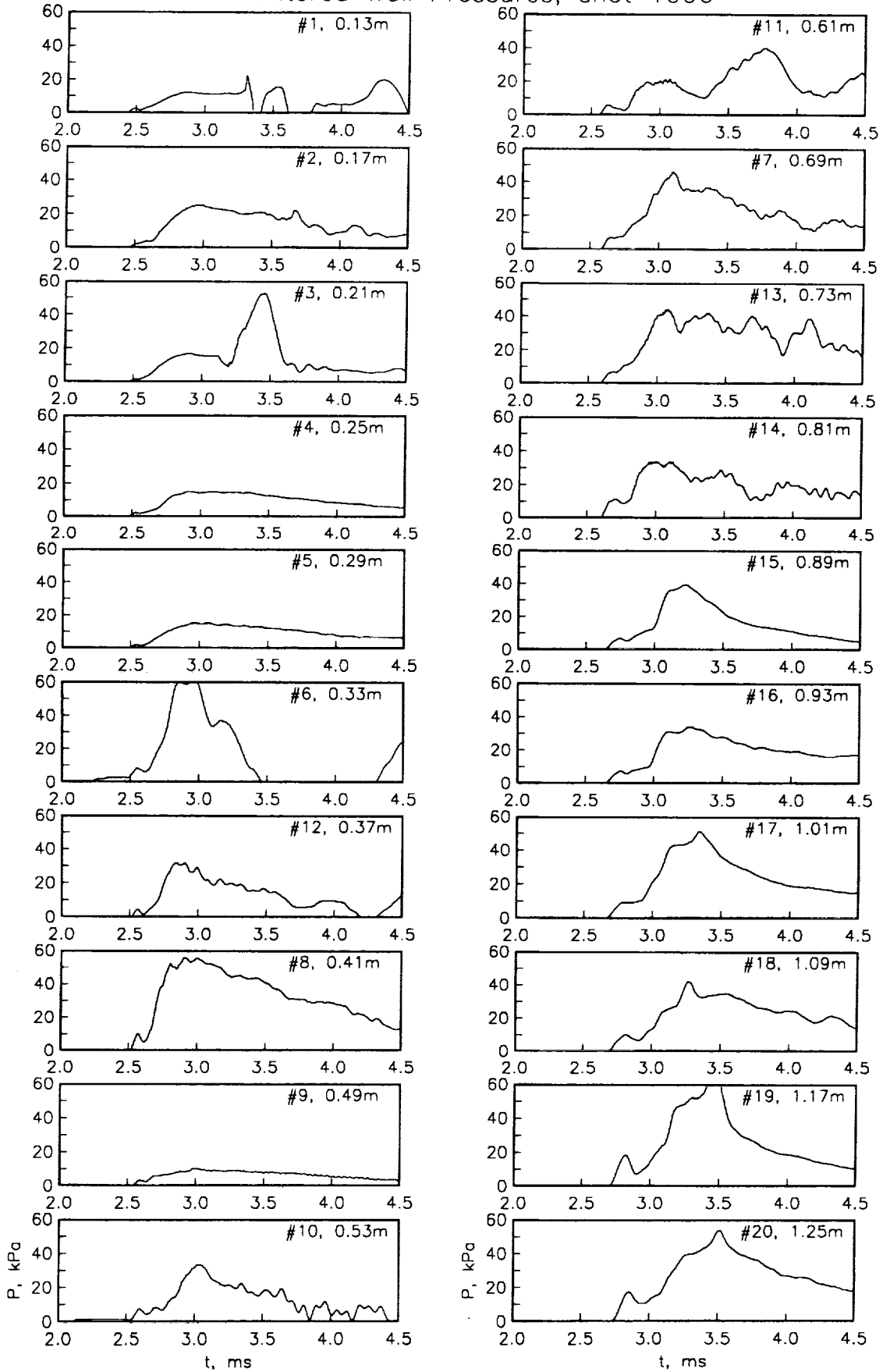
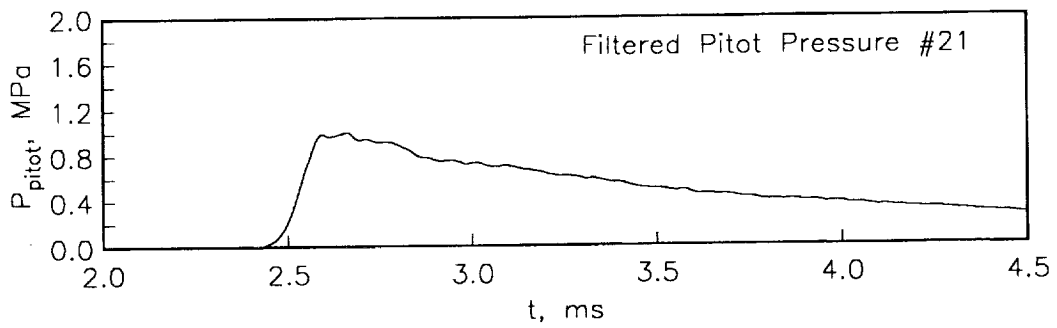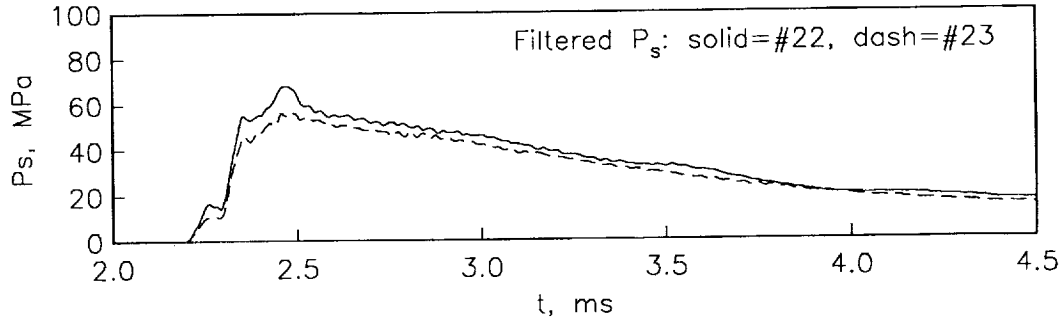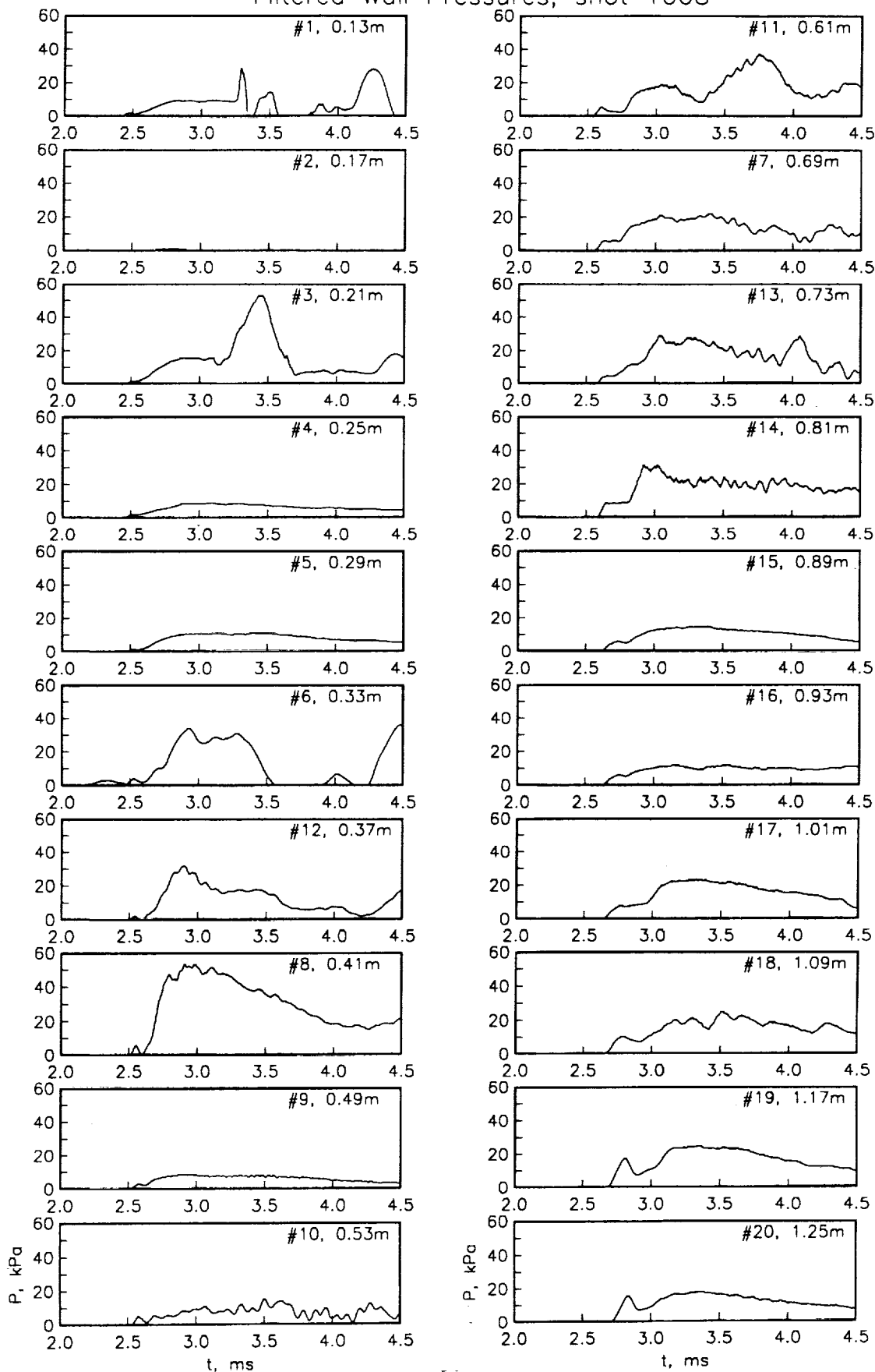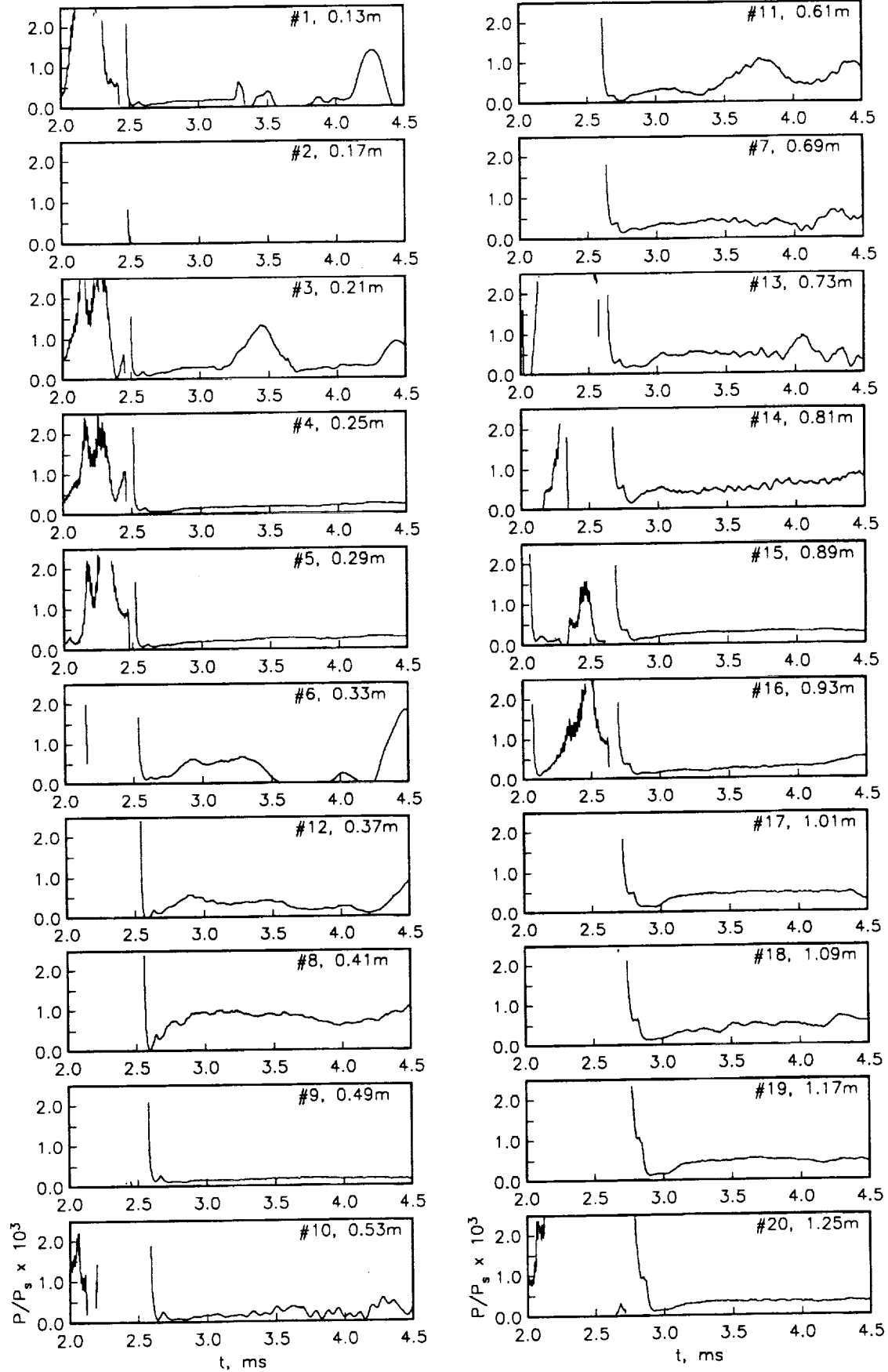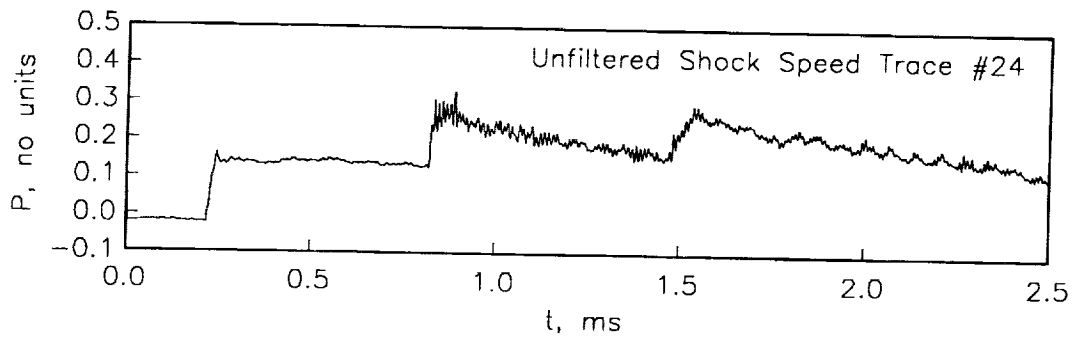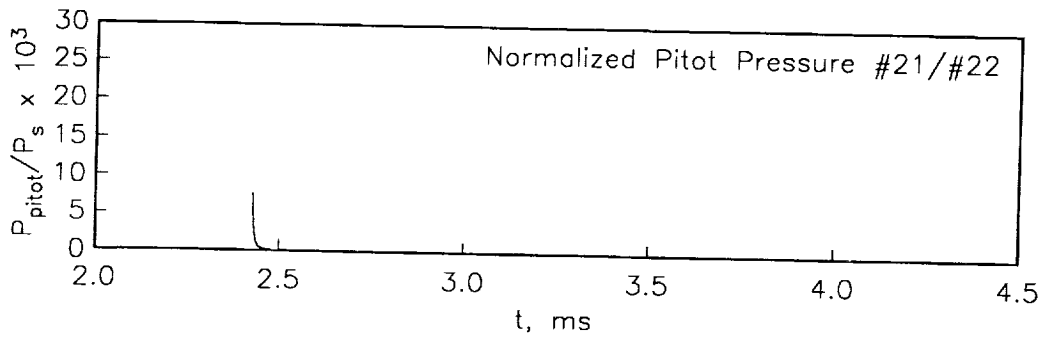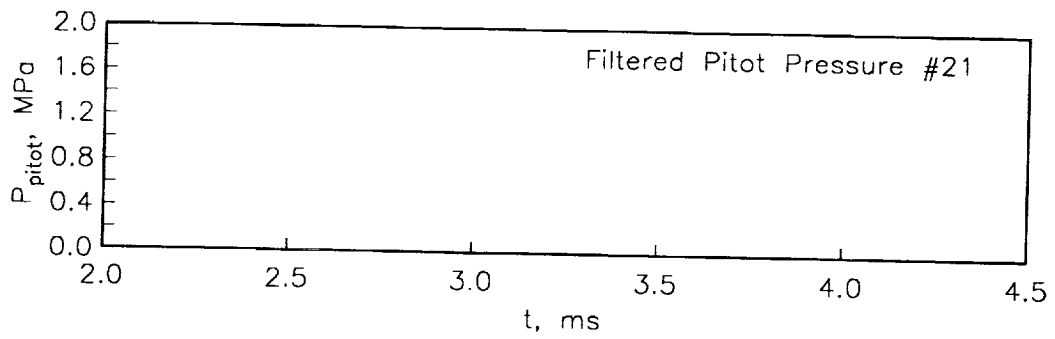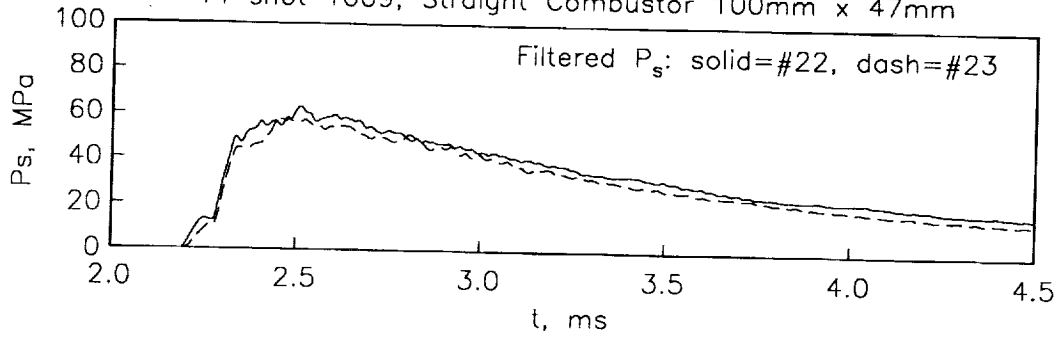Normalized Wall Pressures, shot 1006
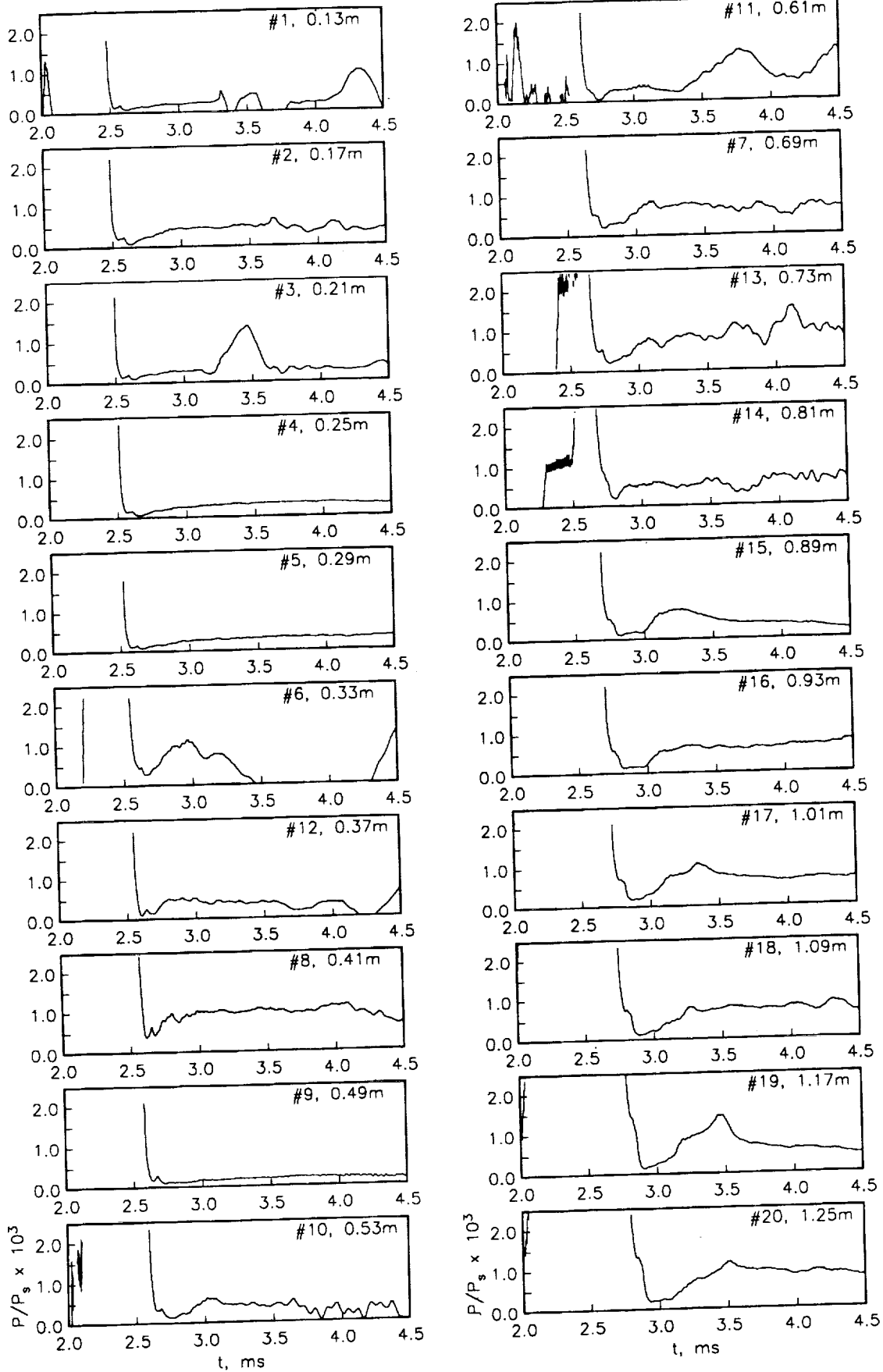
T4 shot 1007, Straight Combustor 100mm x 47mm

Filtered P_s: solid=#22, dash=#23

Filtered Pitot Pressure #21

Normalized Pitot Pressure #21/#22

Unfiltered Shock Speed Trace #24

Filtered Wall Pressures, shot 1007

P, kPa

t, ms

Normalized Wall Pressures, shot 1007

22
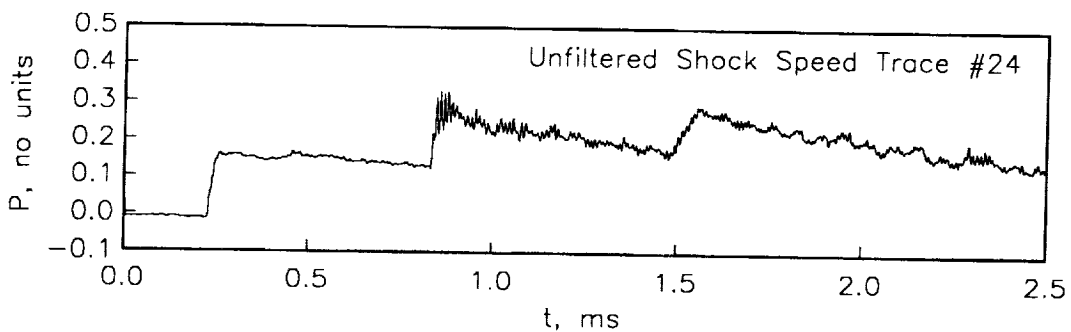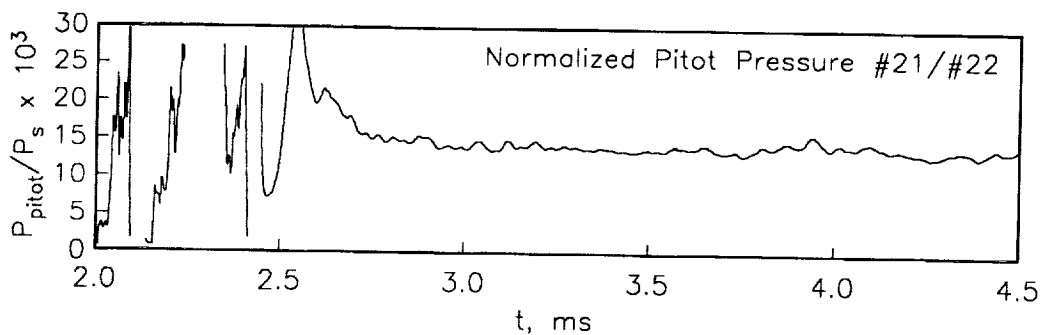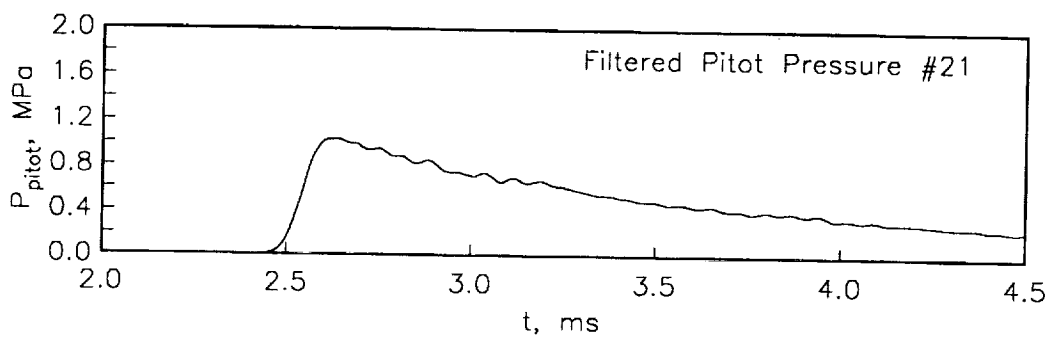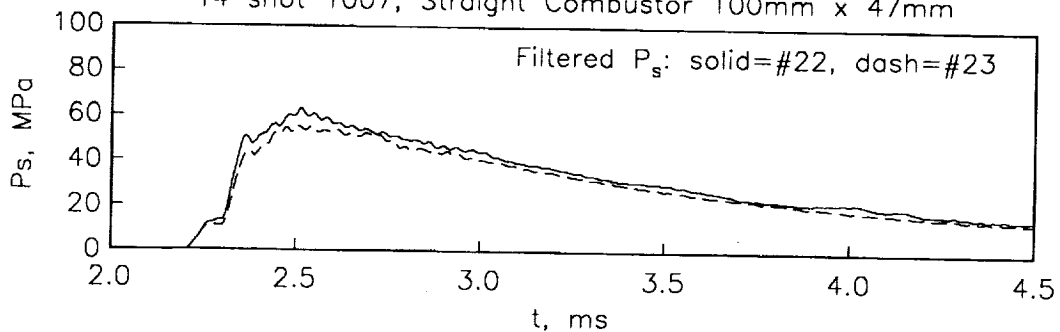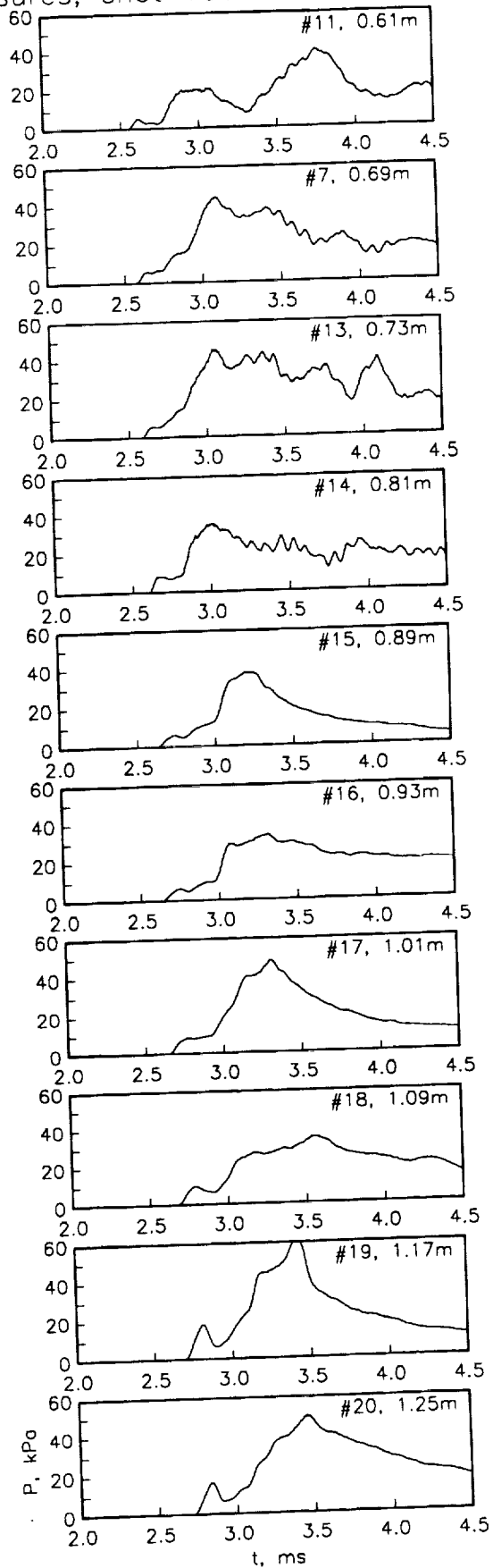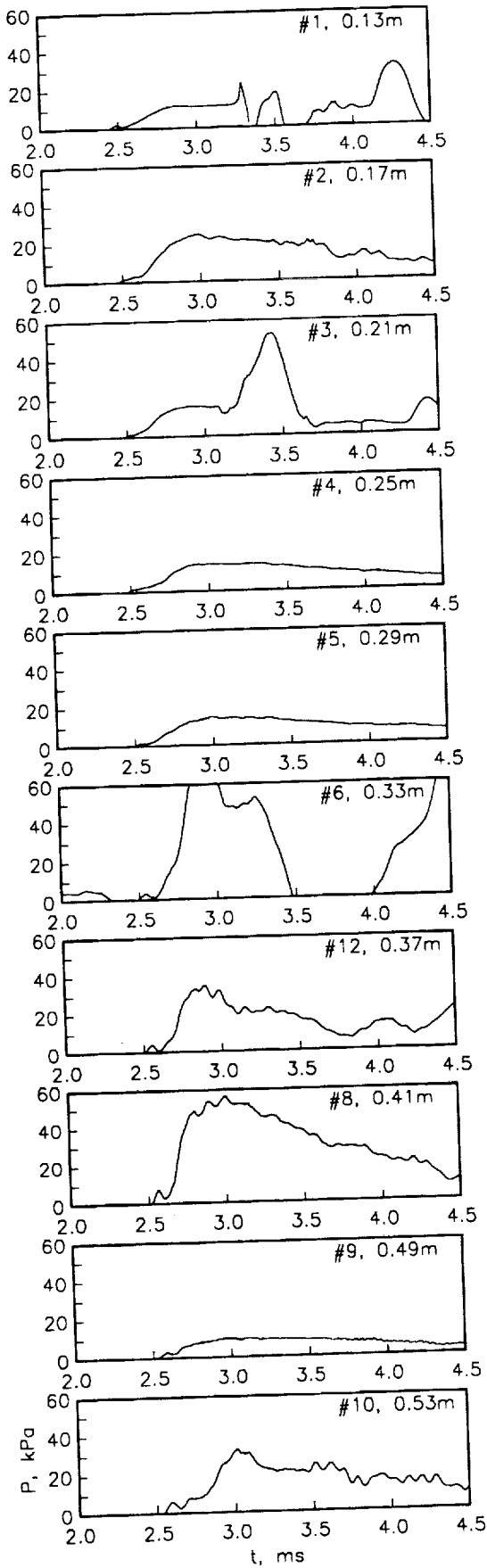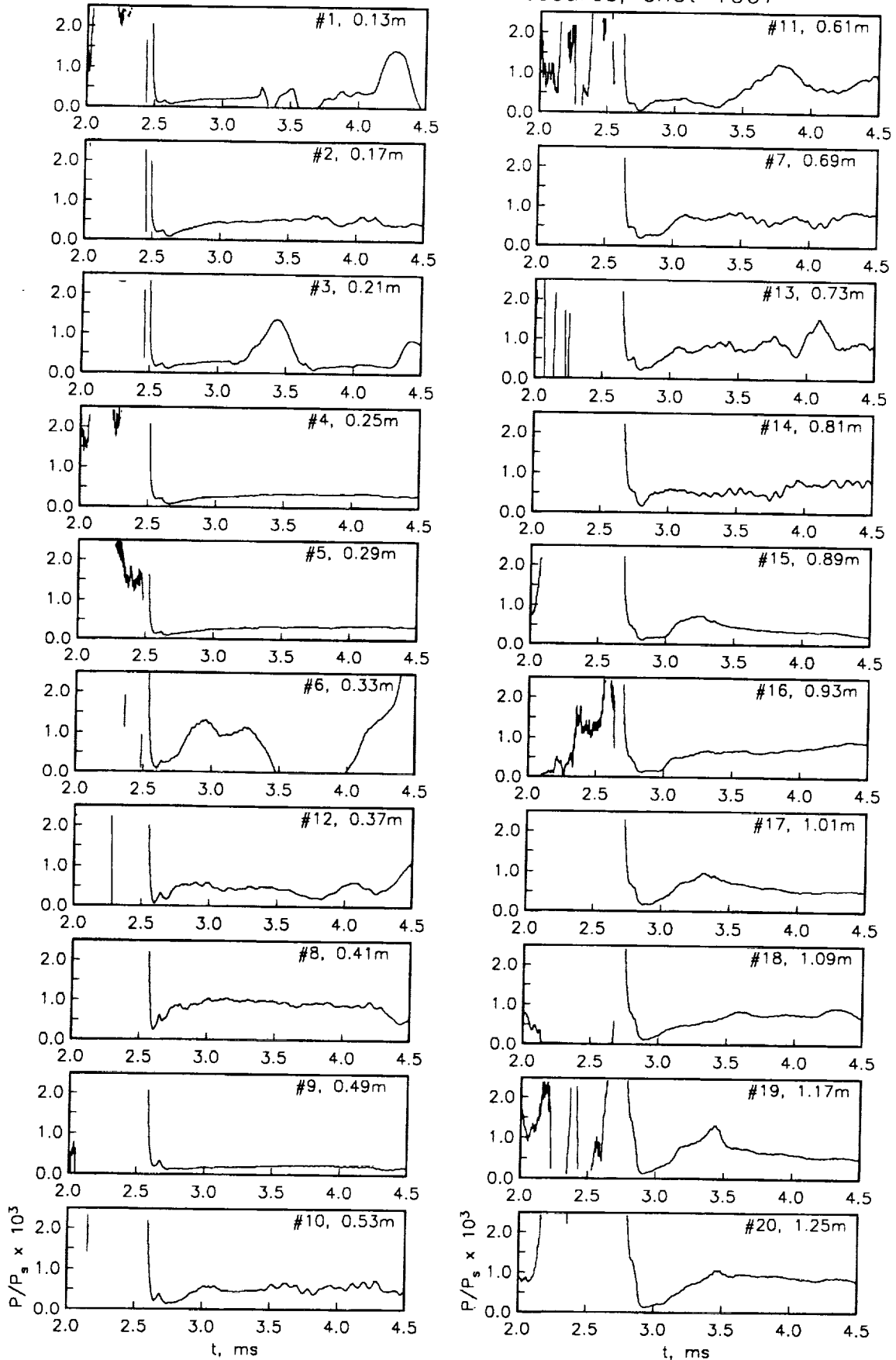
T4 shot 1008, Straight Combustor 100mm x 47mm

Filtered P$_s$: solid=#22, dash=#23

Filtered Pitot Pressure #21

Normalized Pitot Pressure #21/#22

Unfiltered Shock Speed Trace #24

Filtered Wall Pressures, shot 1008
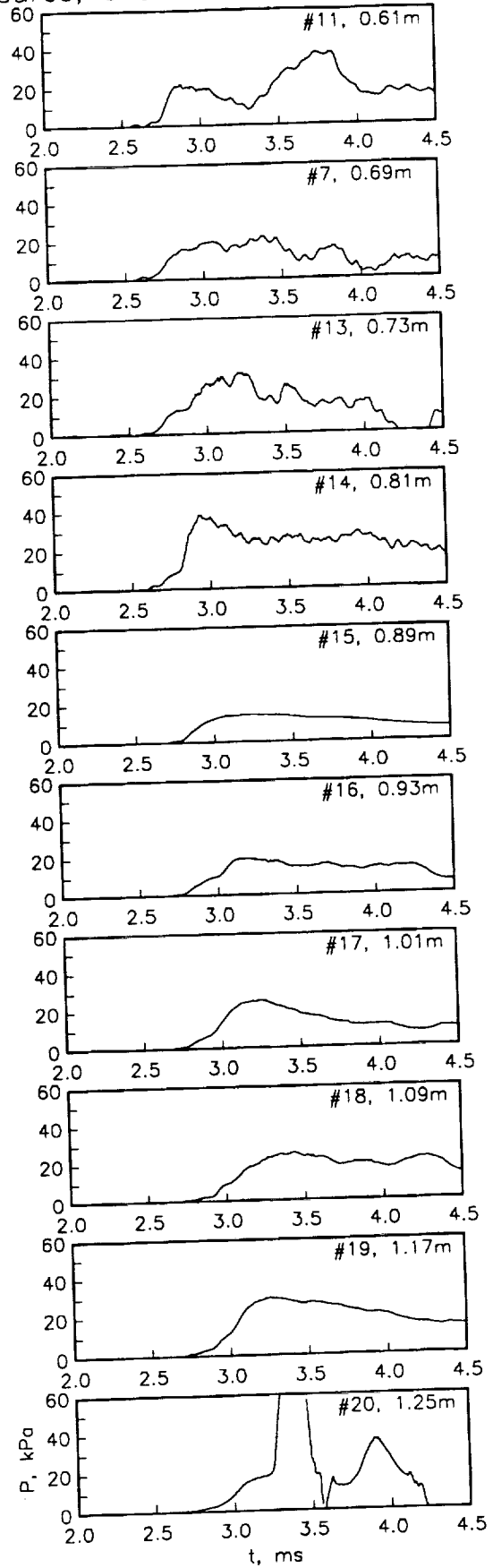

P, kPa

t, ms

Normalized Wall Pressures, shot 1008

25
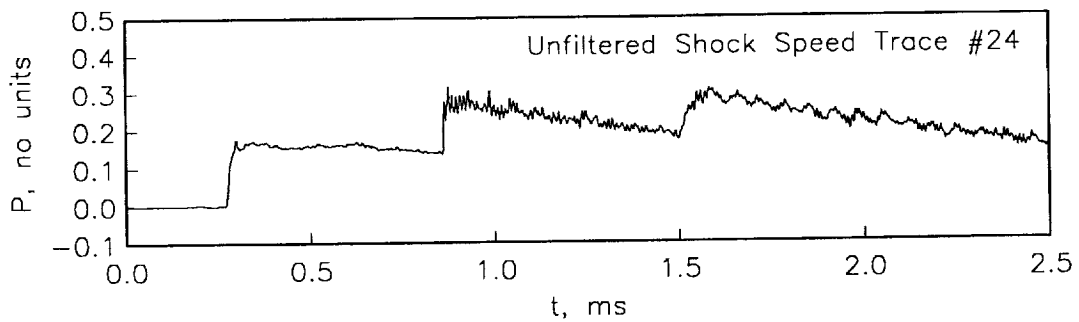
T4 shot 1009, Straight Combustor 100mm x 47mm

Filtered P_s: solid=#22, dash=#23

Filtered Pitot Pressure #21

Normalized Pitot Pressure #21/#22

Unfiltered Shock Speed Trace #24

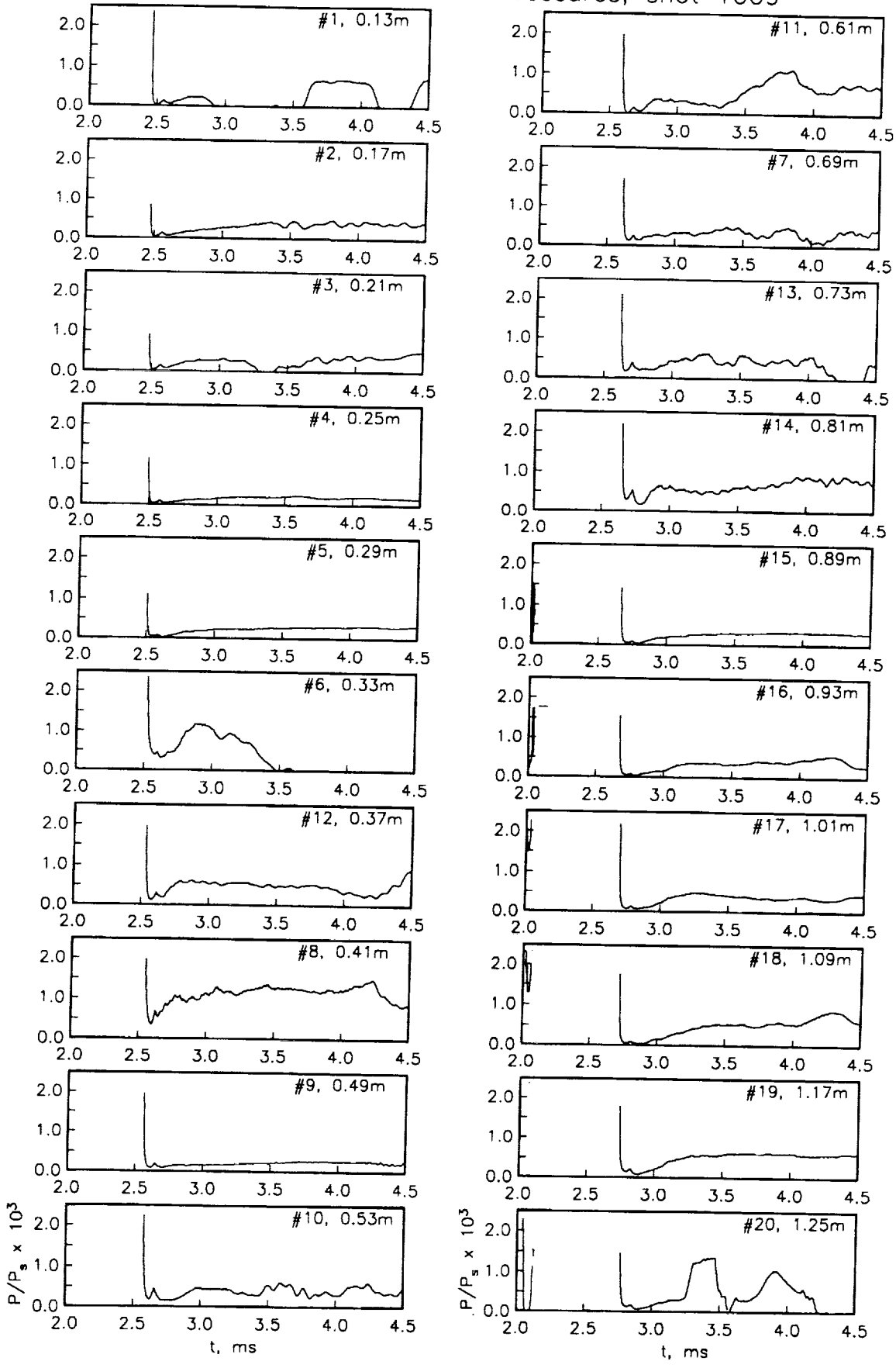Filtered Wall Pressures, shot 1009

27

Normalized Wall Pressures, shot 1009

NASA
National Aeronautics and Space Administration
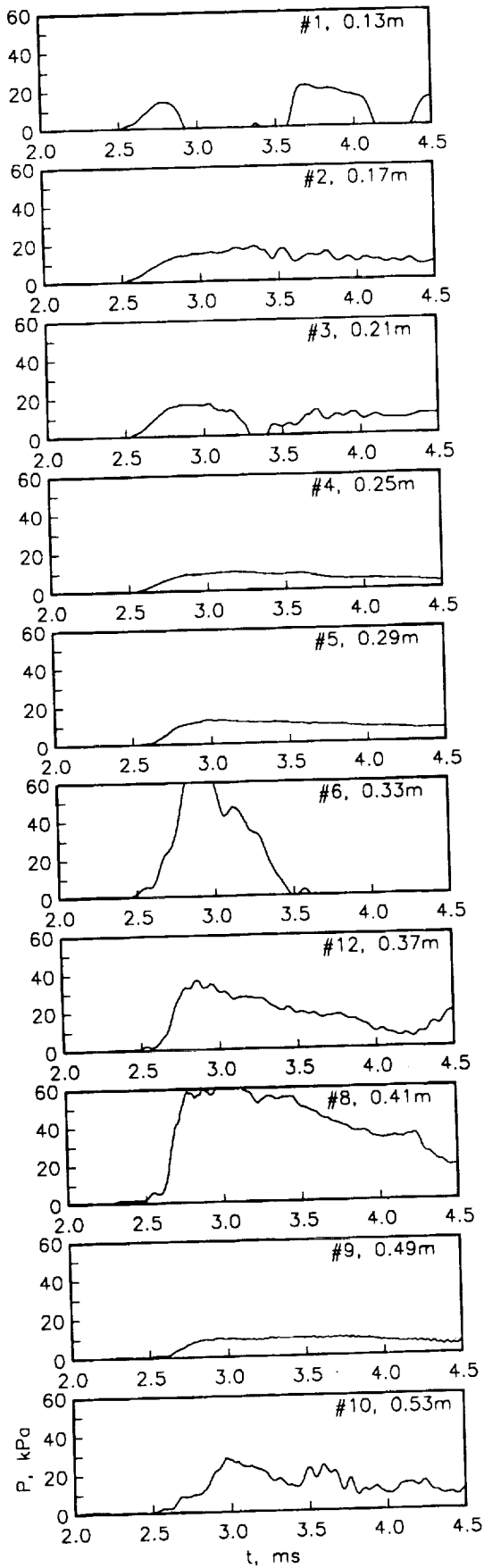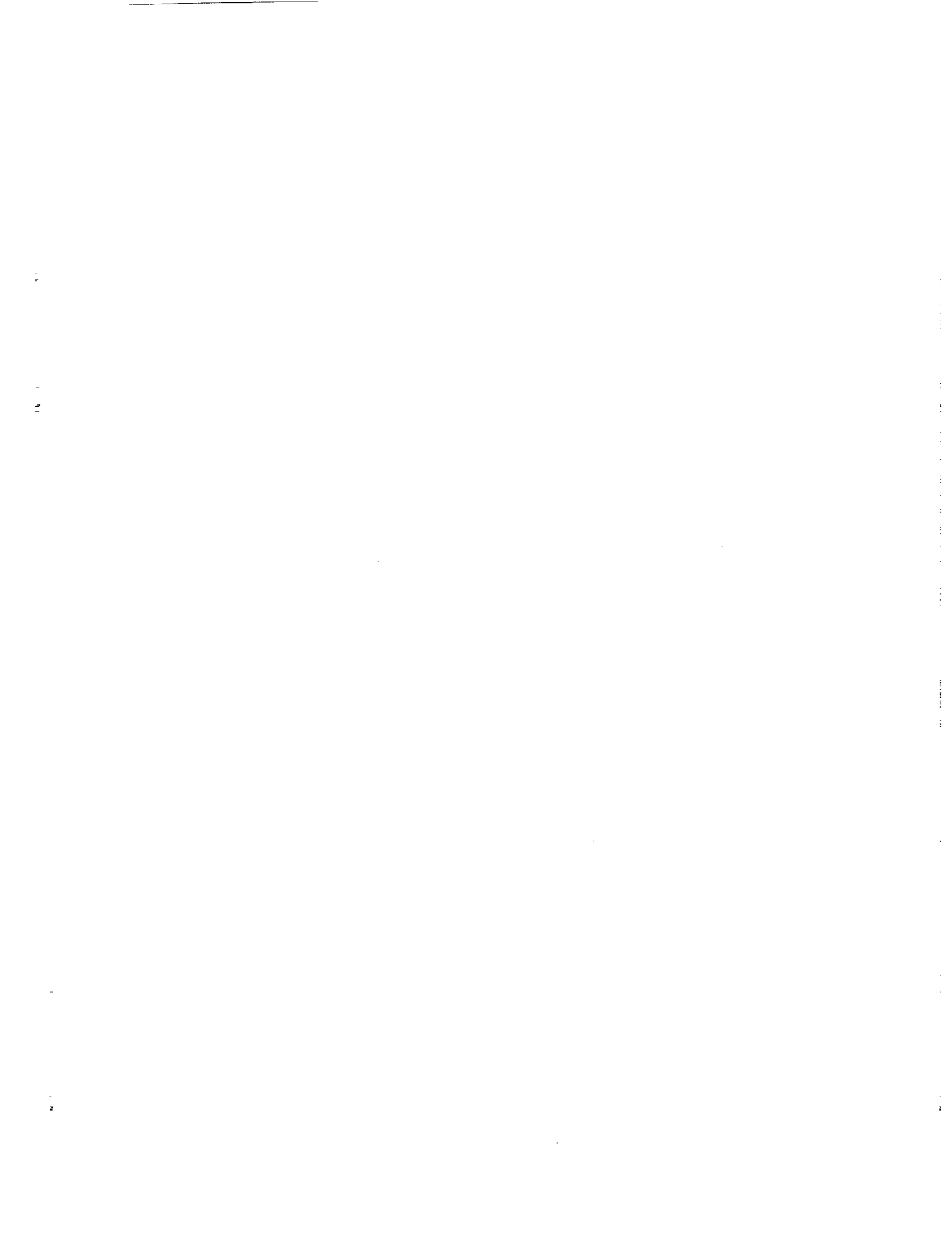
Report Documentation Page

1. Report No. NASA CR-187539 ICASE Interim Report 16	2. Government Accession No.	3. Recipient's Catalog No.

4. Title and Subtitle	5. Report Date
PRELIMINARY CALIBRATION OF A GENERIC SCRAMJET COMBUSTOR	March 1991
	6. Performing Organization Code

7. Author(s) P. A. Jacobs, R. G. Morgan, R. C. Rogers, M. Wendt, C. Brescianini, A. Paull, and G. Kelly	8. Performing Organization Report No. Interim Report No. 16
	10. Work Unit No.

9. Performing Organization Name and Address Institute for Computer Applications in Science and Engineering Mail Stop 132C, NASA Langley Research Center Hampton, VA 23665-5225	505-90-52-01
	11. Contract or Grant No. NAS1-18605
12. Sponsoring Agency Name and Address National Aeronautics and Space Administration Langley Research Center Hampton, VA 23665-5225	13. Type of Report and Period Covered Contractor Report
	14. Sponsoring Agency Code

15. Supplementary Notes

Langley Technical Monitor:
Michael F. Card

Final Report

16. Abstract

The results of a preliminary investigation of the combustion of hydrogen fuel at hypersonic flow conditions are provided. The tests were performed in a generic, constant-area combustor model with test gas supplied by a free-piston-driven reflected-shock tunnel. Static pressure measurements along the combustor wall indicated that burning did occur for combustor inlet conditions of $P_{static} \simeq 19kPa$, $T_{static} \simeq 1080K$ and $U \simeq 3630m/s$ with a fuel equivalence ratio $\phi \simeq 0.9$. These inlet conditions were obtained by operating the tunnel with stagnation enthalpy $H_S \simeq 8.1MJ/kg$, stagnation pressure $P_S \simeq 52MPa$ and a contoured nozzle with a nominal exit Mach number of 5.5.

17. Key Words (Suggested by Author(s)) scramjet, supersonic combustion	18. Distribution Statement 07 - Aircraft Propulsion and Power 34 - Fluid Mechanics and Heat Transfer Unclassified - Unlimited

19. Security Classif. (of this report) Unclassified	20. Security Classif. (of this page) Unclassified	21. No. of pages 32	22. Price A03

NASA FORM 1626 OCT 86